

## Article

# Optical Investigation of 2-amino-7-isocyanofluorene, a Novel Blue-Emitting Solvatochromic Dye

 Bence Kontra <sup>1,2</sup>, Zoltán Mucsi <sup>2,3</sup>, László Vanyorek <sup>3</sup>  and Miklós Nagy <sup>3,\*</sup> 
<sup>1</sup> Department of Organic Chemistry, Semmelweis University, Hógyes Endre utca 7, H-1092 Budapest, Hungary; bence.kontra@femtonics.eu

<sup>2</sup> Brain Vision Center, Department of Chemistry, Vendel utca 9, H-1094 Budapest, Hungary; zoltanmucsi@gmail.com

<sup>3</sup> Institute of Chemistry, University of Miskolc, Miskolc-Egyetemváros, H-3515 Miskolc, Hungary; kemvanyi@uni-miskolc.hu

\* Correspondence: nagy.miklos@uni-miskolc.hu

**Abstract:** Smart solvatochromic isocyano-aminoarenes (ICAAs) have been gaining attention owing to their unique photophysical, antifungal and anticancer properties. Using a simple dehydration reaction with in situ-generated dichlorocarbene, we prepared 2-amino-7-isocyanofluorene (2,7-ICAF). We studied the effect of the longer polarization axis provided by the fluorene core on the spectral properties and we also compared it to those of the starting diamine. 2,7-ICAF shows a clear solvatochromic behavior close to the blue part (370–420 nm) of the visible spectrum. Quantum chemical calculations show internal charge transfer (ICT) between the donor amino and the electron-withdrawing isocyano groups. 2,7-ICAF has high molar absorptivity ( $\epsilon = 15\text{--}18 \cdot 10^3 \text{ M}^{-1}\text{cm}^{-1}$ ) and excellent quantum yield ( $\Phi_f = 70\text{--}95\%$ ) in most solvents; however, its fluorescence is completely quenched in water. The high brightness ( $\epsilon \cdot \Phi_f$ ) and close to zero quantum yield in water may be favorable in biolabeling applications, where background fluorescence should be kept minimal. Overall, 2,7-ICAF shows enhanced photophysical properties compared to its previously investigated relative 4-amino-4'-isocyano-1,1'-biphenyl (4,4'-ICAB).

**Keywords:** isocyanide; fluorene; solvatochromic; fluorescence; dye



**Citation:** Kontra, B.; Mucsi, Z.; Vanyorek, L.; Nagy, M. Optical Investigation of 2-amino-7-isocyanofluorene, a Novel Blue-Emitting Solvatochromic Dye. *Colorants* **2024**, *3*, 86–98. <https://doi.org/10.3390/colorants3020006>

Academic Editor: Julien Massue

Received: 30 November 2023

Revised: 26 January 2024

Accepted: 12 March 2024

Published: 25 March 2024



**Copyright:** © 2024 by the authors. Licensee MDPI, Basel, Switzerland. This article is an open access article distributed under the terms and conditions of the Creative Commons Attribution (CC BY) license (<https://creativecommons.org/licenses/by/4.0/>).

## 1. Introduction

Development of high-performance environment-sensitive dyes [1] and/or fluorescent solvatochromic [2–4] probes are one of the main focuses of today's material science. The solvatochromic behavior of these dyes is usually attributed to an intramolecular charge transfer (ICT) [5] between an electron-donating (D) and an electron-withdrawing (A) group placed on an aromatic core. Upon excitation, due to the shift of electron density from the donor to the acceptor group mediated by the  $\pi$ -linker moiety, the excited state dipole moment ( $\mu_e$ ) usually increases compared to that of the ground state ( $\mu_g$ ). In the excited state ( $S_1$ ), solvent molecules rearrange around the dye, thereby stabilizing it and lowering its energy. This phenomenon is called positive solvatochromism and is characteristic of push–pull type dyes, where the wavelength of the emitted light is shifted bathochromically (towards red) in polar solvents. One of the most published members of this group is naphthalene-based [1-(6-(dimethylamino)-naphthalen-2-yl)propan-1-one], or 2,6-PRODAN [6].

When we exchange the strong electron-withdrawing carbonyl group of PRODAN to the more versatile isocyano group we get isocyano-aminoarenes, our current field of interest. The first member of this dye family prepared by Nagy et al. was 1-amino-5-isocyanonaphthalene, or 1,5-ICAN (Figure 1) [7]. Surprisingly, 1,5-ICAN has the same solvatochromic range as 2,6-PRODAN despite the weaker electron-withdrawing nature of the isonitrile group ( $-\text{N}\equiv\text{C}$ ) and the lower electron-donating ability of the  $\text{NH}_2$  group compared to that of  $\text{N}(\text{CH}_3)_2$ . The excellent complexation property of the isonitrile group

can be utilized in biolabeling and  $\text{Ag}^+$  detection [8]. In addition, the  $-\text{N}\equiv\text{C}$  group reacts selectively with  $\text{Hg}^{2+}$ , making 1,5-ICAN the simplest fluorophore for the ratiometric detection of  $\text{Hg}^{2+}$  ions [9].

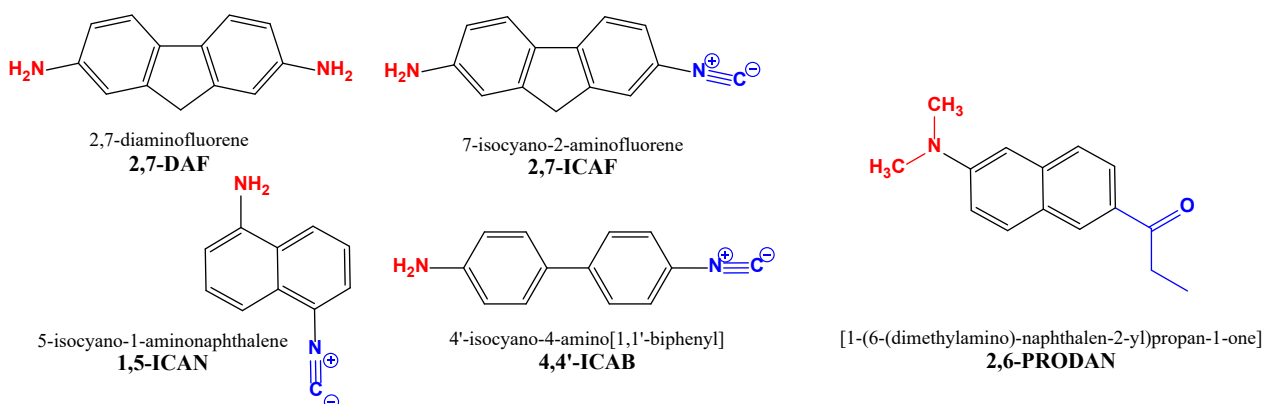


**Figure 1.** The isocyano-aminoarene-type push–pull fluorophores (2,7-ICAF, 1,5-ICAN and 4,4'-ICAB), the starting material (2,7-DAF) and a commercially available dye (2,6-PRODAN) for comparison.

The electronic absorption spectra for the naphthalene-based PRODAN analogues [10–12] and our ICAN derivatives are located in the UV spectral region, which limits their biological applicability. To overcome this issue, one may use two-photon excitation [13], or more favorably the exchange of the fluorochromic core, this way increasing the polarization axis and the dipole moment change of the dye. Using the second approach to enhance the optical properties of the PRODAN and ICAN families, pyrene [14], anthracene (Anthradan) [15,16] and acridine (2,7-ICAAC) [17] derivatives were also prepared from both dye families. Indeed, the solvatochromic range was significantly redshifted and the isocyanoacridine derivatives turned out to be promising photodynamic anticancer agents [17]. We also tried the biphenyl core (4,4'-ICAB, Figure 1) [18]; however, owing to the free rotation of the two benzene rings with respect to each other, the otherwise significant solvatochromic range (409–513 nm for 1,5-ICAN [7]) blueshifted to 350–450 nm.

Using a fluorene ring instead of biphenyl could solve the rotation problem and could provide the enlarged polarization axis required. Indeed, fluorene is used in various applications, such as light-emitting organic diodes (OLEDs) [19], lasing materials [20], in positron emission tomography (PET) [21] and as highly emissive fluorescent molecules with aggregate fluorescence change [22]. Most importantly, it was demonstrated previously that the substitution of the naphthalene core to fluorene in the case of PRODAN led to a 200 nm wider solvatochromic range (FR0 and FR8) [23]. In addition, 2-amino-7-nitrofluorene (ANF) [24,25] is an excellent solvatochromic dye. ANF is still widely used in scientific research to study the mechanisms of carcinogenesis and DNA damage [26].

Based on the above, we wanted to develop improved, redshifted solvatochromic dyes based on ICAN using the fluorene core as the  $\pi$ -linker. One of the main advantages of ICAN derivatives is their cheap and simple synthesis. Using in situ generated dichlorocarbene ( $:\text{CCl}_2$ ) in basic solution [7], one or both amino groups of the respective aromatic diamine is converted to isocyanide. Despite their simple preparation and unique photophysical properties, the field of fluorescent isocyano-aminoarenes remains largely unexplored.

In this paper, we report the synthesis and investigation of 2-amino-7-isocyano fluorene (2,7-ICAF, Figure 1). The photophysical properties of 2,7-ICAF are compared to those of the starting 2,7-diaminofluorene (2,7-DAF) and the very similar 4-amino-4'-isocyanobiphenyl (4,4'-ICAB).

## 2. Materials and Methods

### 2.1. Materials

2,7-Diaminofluorene dihydrochloride (CAS Number: 13548-69-1, MW = 269.176 g/mol) and benzyltriethylammonium chloride (CAS Number: 56-37-1, 99%, MW = 227.77 g/mol) were purchased from Sigma Aldrich (Schnellendorf, Germany) and were used as received. Tetrahydrofuran (THF), methanol (MeOH), dimethyl sulfoxide (DMSO), dichloromethane (DCM) (for Spectroscopy, Sigma Aldrich, Schnellendorf, Germany), toluene (anhydrous, reagent grade, Sigma Aldrich, Germany), acetonitrile, water (HPLC grade, VWR, Darmstadt, Germany), acetone (anhydrous, reagent grade, VWR, Darmstadt, Germany) and ethyl-acetate (EtOAc) (reagent grade, Molar Chemicals, Halásztelek, Hungary) were used without further purification. Other solvents and reagents were purchased from Sigma Aldrich in reagent grade and used as received.

### 2.2. Synthesis of 2-amino-7-isocyanofluorene (2,7-ICAF)

A total of 400 mg 2,7-diaminofluorene dihydrochloride (1.5 mmol; 1.0 eq.) was dissolved in 3.4 mL CH<sub>2</sub>Cl<sub>2</sub> in a small 25 mL round bottom flask, then 0.36 mL chloroform (4.5 mmol, 532 mg, 3 eq.) and 3 mg benzyltriethylammonium chloride (0.01 mmol, 0.01 eq.) were added. The slow addition of 3.4 mL of 50% NaOH solution (42.2 mmol, 28.4 eq.) followed with vigorous stirring. The reaction mixture was stirred at room temperature for 10 min, then stirred at 40 °C with gentle refluxing for 2 h. The reaction was followed by High Pressure Liquid Chromatography with Mass Spectrometer detection (HPLC-MS). After two hours the decomposition of the product was observed, and the reaction mixture was processed in a separatory funnel. A total of 10 mL CH<sub>2</sub>Cl<sub>2</sub> was added, and the phases were separated. The aqueous phase was washed twice with 10 mL CH<sub>2</sub>Cl<sub>2</sub>. The combined organic phases were dried on MgSO<sub>4</sub>, then evaporated on a rotary evaporator. 2,7-ICAF was purified on normal phase silica column (2 × 25 g flash cartridge) using pure dichloromethane as eluent. Pure product: yellow crystals, 38 mg, 9.5% yield.

Melting point: 156 °C (decomposed).

<sup>1</sup>H NMR (400 MHz, DMSO-d<sub>6</sub>) δ = 7.66 (d, J = 8.1 Hz, 1H, C<sub>10</sub>), 7.61–7.54 (m, 2H, C<sub>1</sub>), 7.43 (dd, J = 8.1, 2.0 Hz, 1H, C<sub>11</sub>), 6.76 (d, J = 2.1 Hz, 1H, C<sub>4</sub>), 6.60 (dd, J = 8.2, 2.1 Hz, 1H, C<sub>6</sub>), 5.41 (s, 2H, C<sub>14</sub>), 3.77 (s, 2H, C<sub>9</sub>) (Figure S1).

<sup>13</sup>C NMR (101 MHz, DMSO-d<sub>6</sub>) δ = 162.9 (C<sub>16</sub>), 149.5 (C<sub>5</sub>), 145.6 (C<sub>3</sub>), 143.8 (C<sub>7</sub>), 142.9 (C<sub>8</sub>), 127.8 (C<sub>2</sub>), 125.1 (C<sub>11</sub>), 122.6 (C<sub>10,13</sub>), 121.6 (C<sub>1,12</sub>), 113.1 (C<sub>6</sub>), 109.9 (C<sub>4</sub>), 36.1 (C<sub>9</sub>) (Figure S2).

2D (COSY, HSQC and HMBC) NMR spectra are presented in Figures S3–S5.

### 2.3. Characterization Methods

**LCMS:** The reactions were monitored by a Shimadzu LC-40D XR UPLC-MS system equipped with an SIL-40C XR autosampler, an SPD-M40 photo diode array detector and an LCMS-2020 DUIS Mass Spectrometer operated in negative and positive ionization modes. The separation was carried out on an Ascentis<sup>®</sup> Express C18 with a 2 μm UHPLC column (L × I.D. 5 cm × 2.1 mm) at 50 °C provided by a CTO-40s column oven. Gradient elution was used with either eluent: 0.1% TFA in water (A) and 0.1% TFA in MeCN (B), or 0.4 g NH<sub>4</sub>HCO<sub>3</sub> in 1 L water (A) and MeCN (B).

**Flash Chromatography:** Reaction products were purified by flash column chromatography using an Interchim puriFlash xs 520 plus system on normal phase silica gel columns using isocratic elution (DCM as eluent).

**m.p.:** The melting point was determined on a Büchi M-560 capillary melting point apparatus and was uncorrected.

**UV-vis:** For recording the absorption spectra, a UV-6300PC double beam spectrophotometer (VWR International) was used. Solutions of 3.00 cm<sup>3</sup> were prepared from the sample in the solvent of interest in a quartz cuvette of 1.00 cm optical length. Molar absorption coefficients (ε) were calculated from the absorbance measurements at 3 different concentrations (1×, 2× and 3×, respectively) using the Beer–Lambert law.

Steady-state fluorescence spectra were recorded on a Jasco FP-8550 fluorescence spectrophotometer at 20 °C. The excitation and emission bandwidths were both set to 2.5 nm. To obtain better resolution, 200 nm/min scanning speed was applied for all samples. Fluorescence quantum yields ( $\Phi_F$ ) were calculated by using quinine sulfate in 0.1 mol/L perchloric acid, absolute quantum efficiency ( $\Phi_r = 60\%$ ) [27] as the reference using the method detailed in Ref [27]. The absorbances at the wavelength of excitation were kept below  $A = 0.1$  in order to avoid inner filter effects.

For UV-vis and fluorescence measurements, the investigated compounds were dissolved in acetonitrile at a concentration of 0.6 mg/mL and were diluted to  $7.40 \times 10^{-6}$  M (2,7-DAF) or  $4.84 \times 10^{-6}$  M (2,7-ICAF) in the solvents of interest.

The NMR spectra were recorded at 25 °C, in the solvent indicated, on a Varian Mercury Plus spectrometer (Agilent Technologies, Santa Clara, CA, USA) at a frequency of 400 MHz ( $^1\text{H}$ ) or 101 MHz ( $^{13}\text{C}$ ). Notations for the  $^1\text{H}$  NMR spectral splitting patterns include singlet (s), doublet (d), triplet (t), broad (br) and multiplet/overlapping peaks (m). Chemical shifts of the resonances are given as  $\delta$  values in ppm and coupling constants (J) are expressed in Hertz.

#### 2.4. Density Functional Theory (DFT) Calculations

Theoretical calculations were carried out by Gaussian16 software [28] using the standard convergence criteria given as default. Optimization and vibrational frequencies were carried out by the B3LYP method [29,30] using the 6-311++G(2d,2p) basis set and the IEFPCM method for implicit solvent models. Thermodynamic functions were computed at 298.15 K. For wavelength prediction, the vertical excitation was modelled by the TD-B3LYP/6-311++G(2d,2p)//PCM(DMSO) [31] level of theory using the geometries optimized from B3LYP/6-311++G(2d,2p)//PCM(DMSO). The emission wavelengths were calculated after optimization using the geometries provided by TD-B3LYP/6-311++G(2d,2p)//PCM(DMSO).

### 3. Results and Discussions

#### 3.1. Synthesis of 2-amino-7-isocyanofluorene (2,7-ICAF)

To make a classical push-pull-type dye from symmetrical 2,7-diaminofluorene (2,7-DAF), one of the electron donor amino groups was converted to an electron-withdrawing isocyanide group using the simple dichlorocarbene reaction (Figure 2). This simple reaction requires mild conditions, it is cheap and the unreacted diamine can be easily recovered.

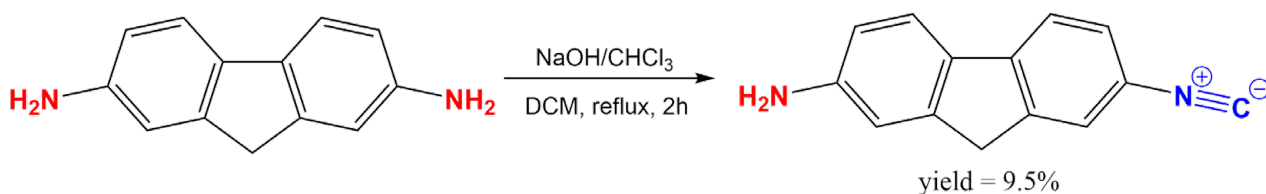


**Figure 2.** The synthesis of 2-amino-7-isocyanofluorene (2,7-ICAF) from 2,7-diaminofluorene (2,7-DAF).

#### 3.2. Optical Characterization of 2,7-diaminofluorene (2,7-DAF) and 2-amino-7-isocyanofluorene (2,7-ICAF)

To investigate the photophysical properties, absorption (UV-vis) and steady-state emission spectra of the starting diamine 2,7-DAF and the isocyanide derivative 2,7-ICAF were recorded in various solvents. The main aspects considered during solvent selection were that they should cover the widest polarity range and contain both H-bond donor and acceptor solvents. This way, in addition to polarity-induced spectral effects, possible specific dye-solvent interactions could also be explored. It should be noted here that we encountered serious solubility issues for 2,7-ICAF; therefore, we had to skip measurements in hexane.

The absorption (UV-vis) and steady-state fluorescence spectra of 2,7-DAF and 2,7-ICAF recorded in solvents of different polarities are presented in Figure 3. Table 1 summarizes the most important spectral properties, such as absorption maximum wavelengths ( $\lambda_{Abs}$ ), molar absorption coefficients ( $\epsilon$ ) and the emission maxima ( $\lambda_{Em}$ ). The non-normalized spectra are presented in the Supporting Information in Figures S6 and S7.

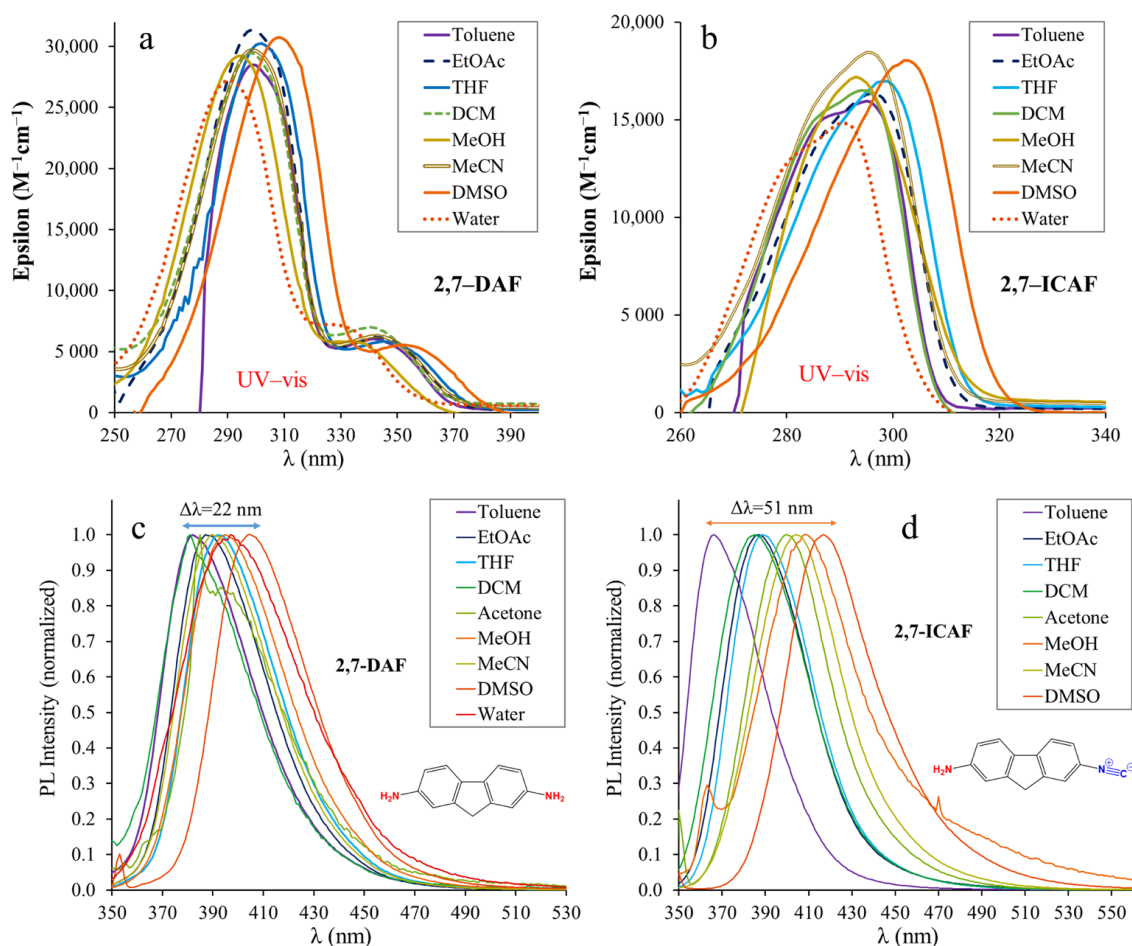


**Figure 3.** The UV-vis absorption (a,b) and emission (c,d) spectra of 2,7-diamino-fluorene (2,7-DAF) and 2-amino-7-isocyano-fluorene (2,7-ICAF) in different solvents ( $[2,7\text{-DAF}] = 7.40 \times 10^{-6}$  M,  $[2,7\text{-ICAF}] = 4.84 \times 10^{-6}$  M,  $T = 20$  °C).

The absorption (UV-vis) spectra of 2,7-DAF show a distinct double band character with a high-intensity peak at  $\lambda_{abs} = 290\text{--}310$  nm depending on the solvent and a lower intensity shoulder located at  $\lambda_{abs} = 327\text{--}353$  nm. Quantum chemical calculations revealed that the higher energy peak can be assigned to the  $S_0\text{--}S_2$  electronic transition, while the shoulder can be assigned to the  $S_0\text{--}S_1$  transition. According to the HOMO-LUMO diagram, both bands in Figure 3a belong to the charge transfer (CT) from the amino groups to the fluorene core. The CT character of these bands is further supported by their large variation with changing solvent polarity. The maxima at the shoulders were used as excitation wavelengths when recording the emission spectra of 2,7-DAF. The emission spectra of 2,7-DAF contain only one band in each solvent and the maxima are found between  $\lambda_{em} = 382\text{--}404$  nm (Table 1), covering only  $\Delta\lambda = 22$  nm solvatochromic range. Interestingly, in water the emission maximum is located lower (397 nm) than in DMSO (404 nm). This may be due to the strong H-bonding between the  $\text{NH}_2$  groups and water molecules. It should be noted here that the fluorescence of 2,7-DAF is strongly quenched in acetone ( $\Phi_f = 0.9\%$ ) and in dichloromethane ( $\Phi_f = 0.3\%$ ).

**Table 1.** The absorption maximum wavelengths ( $\lambda_{\text{Abs}}$ ), molar absorption coefficients ( $\epsilon$ ), fluorescence emission maxima ( $\lambda_{\text{Em}}$ ) and quantum yields ( $\Phi_f$ ) determined in various solvents for 2,7-diamino-fluorene (2,7-DAF), 2-amino-7-isocyano-fluorene (2,7-ICAF) and 4-amino-4'-isocyano-biphenyl (4,4'-ICAB). ( $\epsilon_r$ ) stands for the dielectric constants of the solvents.

Solvent ( $\epsilon_r$ )	2,7-DAF				2,7-ICAF				4,4'-ICAB			
	$\lambda_{\text{Abs}}$ (nm)	$\epsilon \times 10^{-3}$ ( $\text{M}^{-1}\text{cm}^{-1}$ )	$\lambda_{\text{Em}}$ (nm)	$\Phi_f$ (%)	$\lambda_{\text{Abs}}$ (nm)	$\epsilon \times 10^{-3}$ ( $\text{M}^{-1}\text{cm}^{-1}$ )	$\lambda_{\text{Em}}$ (nm)	$\Phi_f$ (%)	$\lambda_{\text{Abs}}$ (nm)	$\epsilon \times 10^{-3}$ ( $\text{M}^{-1}\text{cm}^{-1}$ )	$\lambda_{\text{Em}}$ (nm)	$\Phi_f$ (%)
Toluene (2.38)	341	6.0	382	23	330	15.9	367	95	310	5.4	371	7
EtOAc (6.02)	343	6.2	387	20	332	16.3	387	80	315	6.2	397	6
THF (7.58)	345	5.8	392	18	338	16.9	390	82	319	5.1	396	7
DCM (8.93)	340	7.0	381	1	328	16.5	384	70	307	6.1	390	7
Acetone (20.7)	344	6.1	391	0.3	336	16.5	401	87	329	5.5	407	5
Methanol (32.7)	334	5.8	395	21	326	17.1	411	5	308	4.7	419	1
Acetonitrile (37.5)	343	6.3	390	21	330	18.4	405	82	310	5.9	410	6
DMSO (46.7)	353	5.5	404	43	344	18.0	418	94	318	5.3	436	7
Water (80.1)	327	7.2	397	2	322	14.9	-	-	298	5.1	458	0.1

It is evident from Figure 3b,d that the conversion of one of the  $\text{NH}_2$  groups into isocyano, i.e., breaking the symmetry of 2,7-DAF, has a pronounced effect on the optical properties. The large intensity band around 300 nm completely disappears from the UV–vis spectrum of 2,7-ICAF. The longer wavelength ones (previous shoulder) suffer a slight blueshift of approximately 10 nm and are found between the absorption maxima of the starting diamine and those of the biphenyl reference dye 4,4'-ICAB (Table 1). Surprisingly, the molar absorptivity ( $\epsilon$ ) of these bands increases significantly and are found between 15,000 and 18,000  $\text{M}^{-1}\text{cm}^{-1}$ , almost three times larger than those of 4,4'-ICAB (5000–6000  $\text{M}^{-1}\text{cm}^{-1}$ ), and more than double than in the case of naphthalene-based 1,5-ICAN (4000–8000  $\text{M}^{-1}\text{cm}^{-1}$ ) [7]. The measured absorption maximum and the molar absorption coefficient in DMSO are in good agreement with the calculated ones presented in Figure S11. Pronounced change can also be observed in the case of the emission peaks. Compared to the very narrow ( $\Delta\lambda = 22$  nm) solvatochromic range of 2,7-DAF, the range more than doubles ( $\Delta\lambda = 51$  nm) in the case of 2,7-ICAF from toluene to DMSO. In non-polar solvents, such as toluene, the emission is blueshifted  $\lambda_{\text{em}} = 367$  nm versus 382 nm, and in polar solvents a significant redshift is apparent with an emission at  $\lambda_{\text{em}} = 418$  nm versus 404 nm (Figure 3c,d, Table 1). These emission maximum values are within 10 nm of those measured for the reference compound 4,4'-ICAB. A significant difference can only be observed in the case of very polar solvents, namely DMSO and water. Considering the quantum yields ( $\Phi_f$ ), they are low for the biphenyl derivative and nearly quenched in protic solvents (MeOH,  $\text{H}_2\text{O}$ ) for both derivatives. In the case of 2,7-ICAF, complete quenching was observed in water, therefore the emission maximum could not be determined. Interestingly, in nonprotic solvents the quantum yields of 2,7-ICAF are much higher than those of the starting diamine and the biphenyl derivative. They are found between  $\Phi_f = 70$ –95% (DCM–Toluene). These  $\Phi_f$  values are in good agreement with the calculated oscillator strength of 1.27 for the first excited state ( $S_1$ ) of 2,7-ICAF presented in Figure S12. The high quantum yields in combination with high molar absorptivities result in excellent brightness for 2,7-ICAF. The high brightness and complete quenching in aqueous media may make 2,7-ICAF a potent cell stain as we previously demonstrated with 1,5-ICAN [8]. It should be noted, however, that because of the high energy absorption ( $\lambda_{\text{abs}} = 320$ –340 nm), the application may be limited to dead (fixed) cells.

### 3.3. Investigation of the Solvatochromic Behavior of 2,7-DAF and 2,7-ICAF

One of the most recent methods to quantify the solvatochromic behaviors of 2,7-DAF and 2,7-ICAF is the Catalán scale [32]. This multiple linear regression (MLR) analysis-based procedure can account for the specific solvent–dye interactions. The effect of these specific interactions on spectral parameters, such as emission maxima or Stokes shifts ( $\Delta\nu_{\text{SS}}$ ), is determined using Equation (1):

$$y = y_0 + a_{\text{SA}}\text{SA} + b_{\text{SB}}\text{SB} + c_{\text{SP}}\text{SP} + d_{\text{SdP}}\text{SdP} \quad (1)$$

where the  $y_0$  parameter represents the characteristic property ( $\lambda_{\text{em,max}}$ ,  $\Delta\nu_{\text{SS}}$ ) of the substance under consideration in the absence of a solvent. SA quantitatively measures the empirical ability of the bulk solvent to serve as a hydrogen bond donor to a solute. Similarly, SB quantitatively measures the empirical ability of the bulk solvent to act as a hydrogen bond acceptor or electron pair donor to a solute, forming either a solute-to-solvent hydrogen bond or a solvent-to-solute coordinative bond. SP and SdP denote the solvent polarizability and dipolarity parameters, respectively, which are determined using reference dye molecules. The coefficients a, b, c and d in the equation signify the influence of the respective solvent parameter on the property being investigated. The results are presented in Figure 4a,b (Figure S5a,b) and in Table 2.

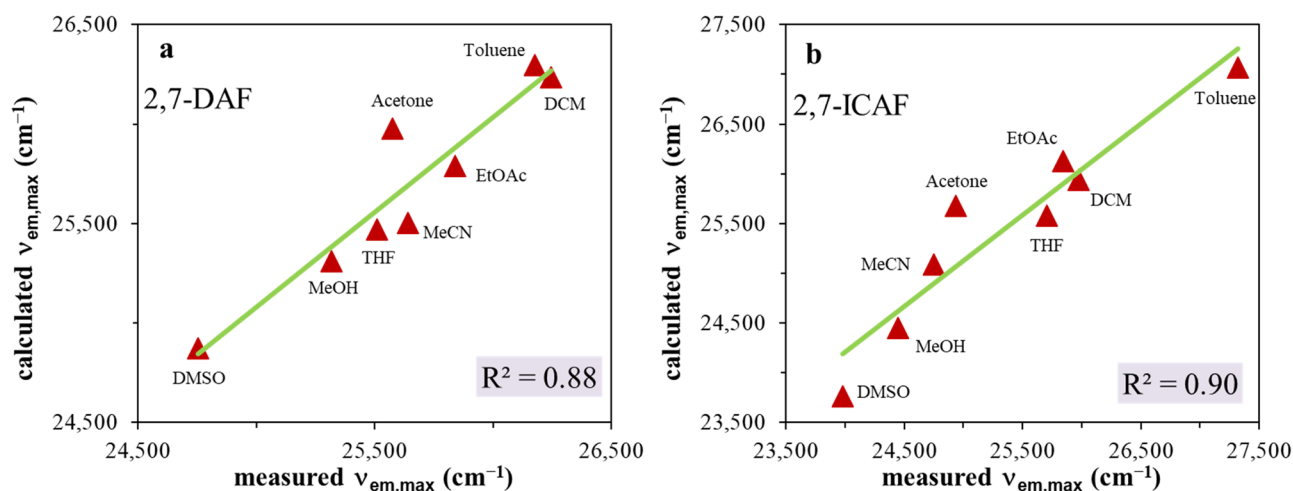


**Figure 4.** Catalán plots for (a) 2,7-diamino-fluorene (2,7-DAF) and (b) 2-amino-7-isocyano-fluorene (2,7-ICAF).

**Table 2.** Correlation coefficients  $a_{SA}$ ,  $b_{SB}$ ,  $c_{SP}$  and  $d_{SDP}$  of the Catalán parameters, solute properties of the reference system (emission maximum,  $\nu_{em,max}$  and Stokes shift,  $\Delta\nu_{ss}$ ), coefficient of determination ( $R^2$ ) and number of solvents ( $n$ ) calculated by MLR analysis for 2,7-DAF and 2,7-ICAF.

		$y_0$ ( $\text{cm}^{-1}$ )	$a_{SA}$	$b_{SB}$	$c_{SP}$	$d_{SDP}$	$R^2$	$n$
2,7-DAF	$\nu_{em,max}$	29,332	−1080	−2340	−3516	51	0.88	8
	$\Delta\nu_{ss}$	2840	2116	551	308	55	0.99	9
2,7-ICAF	$\nu_{em,max}$	32,902	−2184	−2516	−6264	−2155	0.90	8
	$\Delta\nu_{ss}$	1388	3401	9.95	3140	836	0.85	8

As seen in Figure 4a,b, the Catalán equation describes relatively well the change of emission maxima with changing solvent properties. The coefficient of determination is  $R^2 \sim 0.9$  for both 2,7-DAF and 2,7-ICAF. Surprisingly, in the case of the starting diamine, when we plot the calculated Stokes shifts versus the measured ones, an almost perfect fit  $R^2 = 0.99$  was obtained (Figure S5a,b, Table 2). Based on the data of Table 2, the emission maxima of both the diamine (2,7-DAF) and the isocyanide (2,7-ICAF) are determined by the solvent polarizability (large  $c_{SP}$  coefficients), while the H-bond donor character ( $a_{SA}$ ) and polarizability is dominant for the Stokes shifts of 2,7-DAF and 2,7-ICAF, respectively (Table 2).

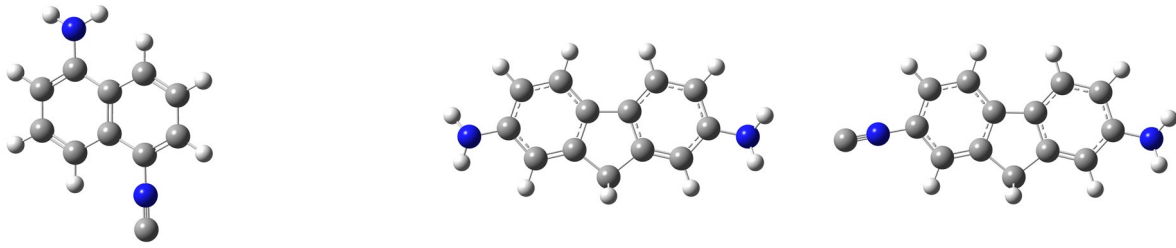
### 3.4. Theoretical Results

To get the whole picture of the photochemical processes and a correct explanation of the experimental findings, theoretical calculations using an implicit IEF-PCM method with the relative permittivity of DMSO were carried out (Figures S9–S12).

The optimized geometries of the ground state ( $S_0$ ) and the first relaxed excited state ( $S_1$ ) of the fluorene derivatives reveal significant changes in the bond lengths of both the donor (amino) and the acceptor (isocyano) groups. In the case of 2,7-DAF, the ground state structure is symmetrical and the C-N bond lengths of the amino groups are 1.40 Å (for both 2- and 7-amino positions), which is characteristic for pyramidal aromatic amines [33]  $C_{Ar}-NH_2$  ( $Nsp^3$ ). The sum of bond angles around the N of the amino group is  $340^\circ$ , which is also characteristic for a pyramidal ( $sp^3$ )  $NH_2$  group. Upon excitation, pronounced changes in the bond lengths take place (Table 3). The C-N (amino) bond length is shortened by almost 0.04 Å to 1.36 Å and the bond pyramidity of the N decreases ( $356^\circ$ ), indicating a more planar,  $sp^2$ -type imino ( $=NH_2^+$ ) group. In the case of the isocyano derivative 2,7-ICAF, the C-N bond length shortens from 1.39 Å ( $S_0$ ) to 1.35 Å ( $S_1$ ) and the angle increases from  $343^\circ$  to  $360^\circ$ , which is characteristic for a completely planar ( $C_{Ar}=NH_2^+$ ) imino form in the

excited state. The 1.36–1.35 Å C-N lengths are characteristic for the planar  $sp^2$  hybridized  $NH_2$  group attached to an aromatic core. According to experimental results [33], the average length is  $d(C_{Ar}-NH_2, N_{sp^2}) = 1.35$  Å. This shortening of the C-NH<sub>2</sub> bond is the result of the electron transfer from the NH<sub>2</sub> group to the NC group, or to the aromatic core in the case of the diamine.

**Table 3.** The ground ( $S_0$ ) and excited states' ( $S_1$ ) geometrical and optical properties of the dyes of interest, calculated for the B3LYP/6-311++G(2d,2p) level in DMSO. Numbers in red represent experimental results. \* The values were taken from Ref. [7].



	1,5-ICAN		2,7-DAF		2,7-ICAF	
	$S_0$	$S_1$	$S_0$	$S_1$	$S_0$	$S_1$
<b>Bond length (Angstrom)</b>						
-NH <sub>2</sub>	1.391	1.340	1.401	1.363	1.392	1.353
$d(C-N)\equiv C$	1.389	1.358	-	-	1.389	1.357
$d(N\equiv C)$	1.167	1.181	-	-	1.167	1.184
$\mu$ (Debye)	7.35	8.61	1.39	1.74	8.84	10.9
abs (nm)	380 (347) *	481 (497) *	339 (353)	392 (404)	343 (347)	406 (417)
NH <sub>2</sub> angle	342	360	340	356	343	360

In the case of the isocyanato group, the bond length between the NC group and the aromatic core also is found around  $d(C_{Ar}-NC) = 1.39$  Å (Table 3,  $S_0$ ), while the length of the triple bond is  $d(N\equiv C) = 1.167$  Å. Significant changes can also be observed for the isocyanato group in the excited state. The  $d(C_{Ar}-NC)$  distance is shortened by about 0.03 Å to 1.36 Å, while the original triple bond is stretched to  $d(N\equiv C) = 1.184$  Å in the excited state, suggesting the presence of a doubly bonded ( $C_{Ar}=N^+=C^-$ ) isocyanato group. These bond length changes are also apparent in our reference compound 1-amino-5-isocyanonaphthalene (1,5-ICAN, Table 3 first column) and indicate a clear charge transfer between the donor NH<sub>2</sub> and the acceptor isocyanato groups. However, the amino group moves closer to the aromatic core in the case of 1,5-ICAN, which has superior solvatochromic properties compared to 2,7-ICAF. The larger distance between the amino and the not so strong acceptor isocyanato groups and the reduced conjugation of the fluorene (and biphenyl) ring may be the explanation for their poorer performance compared to that of 1,5-ICAN.

According to the theoretical study, the biphenyl derivatives (4,4'-DAB and 4,4'-ICAB) represent a simpler vertical excitation in both cases. Here the HOMO→LUMO transition to the first excitation states indicates the dominant process. In the cases of 4,4'-DAB and 4,4'-ICAB, the two phenyl rings rotate towards each other by 30° in the ground state ( $S_1$ ); however, at the  $S_1$  excited state, the rings are located in one plane. For the distorted structure of 2,7-DAF, the absorption band is overlapped by a more complex excitation pattern, and in the case of 2,7-DAF it is represented by the combination of the first and second excited states (Figure 5). The Nucleus Independent Chemical Shift values (NICS) [34,35] of the  $S_0$  and  $S_1$  states also correspond to our chemical expectations. More negative values indicate the more aromatic character for the ring. In the case of diamino derivatives (2,7-DAF and 4,4'-DAB), we observed equivalent chemical shifts, which drop down by at least 1 ppm. In the case of 2,7-ICAF and 4,4'-ICAB, the aromatic ring substituted by an  $-N\equiv C$  group is more aromatic than the aniliny ring. During the excitation, all the NICS values drop down at  $S_1$  states,

showing decreasing aromatic character. This refers to a more quinoidal character for phenyl rings and more stronger interactions and bonds between the two phenyl rings attached, in agreement with the previous observations about bond lengths.

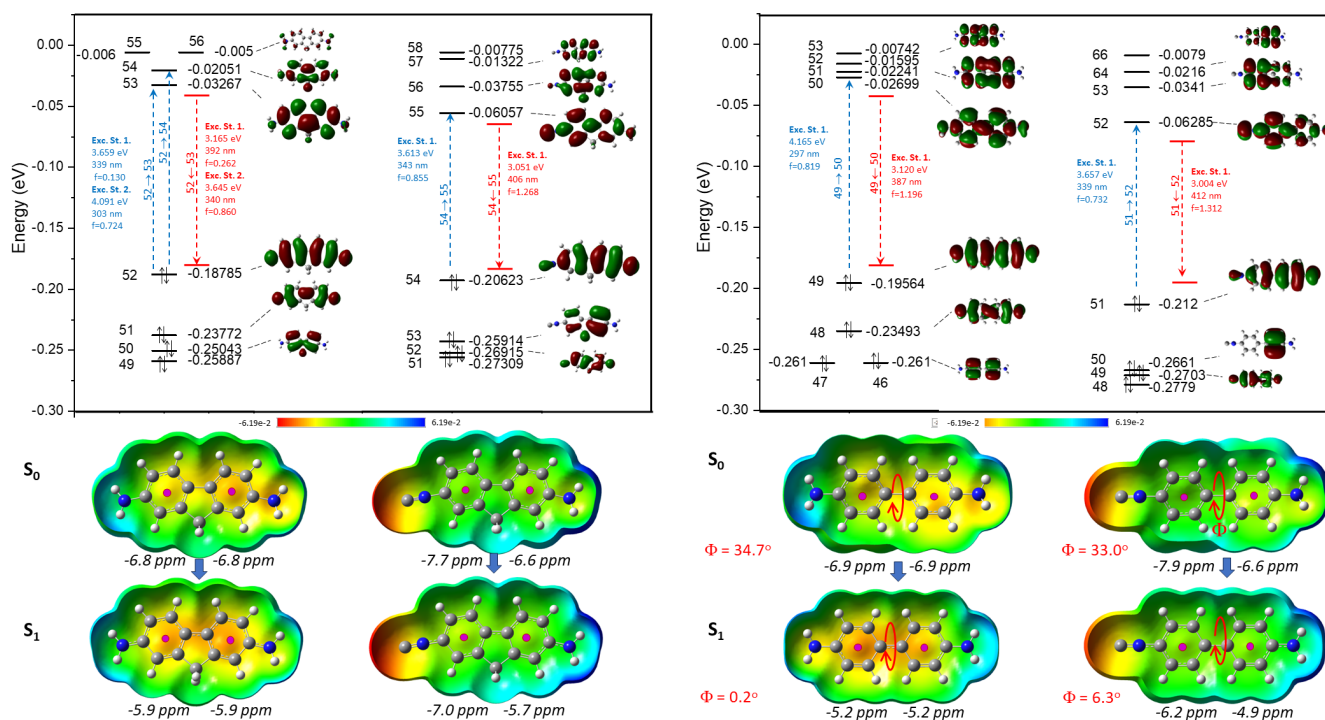


**Figure 5.** Calculated molecular orbitals (MO, above) and electrostatic potential surface ground states ( $S_0$ ) and excited states ( $S_1$ ) (ESP, below) of 2,7-DAF and 2,7-ICAF (left) as well as 4,4'-DAB and 4,4'-ICAB (right), together with the calculated spectroscopical data and the dihedral angles of 4,4'-DAB and 4,4'-ICAB. The black italic numbers are the calculated NICS values for the corresponding aromatic rings.

#### 4. Conclusions

A fluorene core push–pull-type dye, namely 2-amino-7-isocyanofluorene (2,7-ICAF), was synthesized from 2,7-diaminofluorene (2,7-DAF) using a simple dichlorocarbene method in strongly basic solution. The optical properties of both the starting diamine and the isocyano derivative were investigated. Fluorescence spectra revealed the broadening of the solvatochromic range to 51 nm (367–418 nm) for 2,7-ICAF compared to 22 nm for the diamine. However, the emission spectra were still located in the higher end of the UV and the lower blue edge of the visible spectrum. Using the Catalán method, both 2,7-DAF and 2,7-ICAF showed good solvatochromic behavior, with the solvent polarizability being the determining parameter. High level quantum chemical calculations revealed that internal charge transfer (ICT) takes place between the amino and the isocyano groups. The reason for the ICT is the shortening of the amino C–N bond in the excited state and the simultaneous stretching of the isocyano triple bond. This behavior is very similar to that of our previously prepared 4-amino-4'-isocyano-biphenyl (4,4'-ICAB). However, while the emission maxima of the two compounds are within 10 nm, their molar absorptivity and quantum yields differ significantly. 2,7-ICAF has excellent quantum efficiencies ( $\Phi_f = 70\text{--}95\%$ ) and large molar absorption coefficients ( $\epsilon = 16,000\text{--}18,000 \text{ M}^{-1}\text{cm}^{-1}$ ). The resulting brightness is far superior compared to those of 4,4'-ICAB and 1,5-ICAN. In addition, the complete quenching of 2,7-ICAF in aqueous media combined with its high fluorescence in nonpolar media is favorable for staining/biolabeling applications.

**Supplementary Materials:** The following supporting information can be downloaded at: <https://www.mdpi.com/article/10.3390/colorants3020006/s1>, Figure S1:  $^1\text{H}$ -NMR spectrum of 2-amino-7-isocyanofluorene (2,7-ICAF); Figure S2:  $^{13}\text{C}$  NMR spectrum of 2-amino-7-isocyanofluorene (2,7-ICAF); Figure S3: COSY spectrum of 2-amino-7-isocyanofluorene (2,7-ICAF); Figure S4: HSQC spectrum of 2-amino-7-isocyanofluorene (2,7-ICAF); Figure S5: HMBC spectrum of 2-amino-7-isocyanofluorene (2,7-ICAF); Figure S6: Steady-state fluorescence (top) excitation, (bottom) emission spectra of 2,7-DAF recorded in various solvents of different polarity; Figure S7: Steady-state fluorescence (top) excitation, (bottom) emission spectra of 2,7-ICAF recorded in various solvents of different polarity; Figure S8: Catalán plots for the (a) 2,7-diamino-fluorene (2,7-DAF) and (b) 2-amino-7-isocyanofluorene (2,7-ICAF); Figure S9: The optimized geometry of 2,7-DAF in the ground  $S_0$  state calculated on the TD-B3LYP/6-311++G(2d,2p)//PCM(solvent level of theory); Figure S10: The optimized geometry of 2,7-DAF in the first excited  $S_1$  state calculated on the TD-B3LYP/6-311++G(2d,2p)//PCM(solvent level of theory); Figure S11: The optimized geometry of 2,7-ICAF in the ground  $S_0$  state calculated on the TD-B3LYP/6-311++G(2d,2p)//PCM(solvent level of theory); Figure S12: The optimized geometry of 2,7-ICAF in the first excited  $S_1$  state calculated on the TD-B3LYP/6-311++G(2d,2p)//PCM(solvent level of theory).

**Author Contributions:** Conceptualization, M.N. and Z.M.; methodology, M.N. and B.K.; formal analysis, M.N. and L.V.; writing—original draft preparation, M.N. and Z.M.; writing—review and editing, M.N., Z.M. and L.V.; visualization, B.K., M.N., Z.M. and L.V. All authors have read and agreed to the published version of the manuscript.

**Funding:** The project was supported by the TKP2021-NVA-14 and 2020-2.1.1-ED-2022-00208 grants of the National Office of Science, Innovation and Technology (NKFIH), János Bolyai Research Scholarship and National Excellence Program (BO/799/21/7, ÚNKP-22-ME3). On behalf of the Development and mechanistic study of DNA dyes (PI: Ervin Kovács) project, we are grateful for the possibility to use ELKH Cloud [36] which helped us achieve the results published in this paper. This research was also supported by the 2020-1.1.6-Jövő-2021-00009 project supported by the National Research Development and Innovation Fund aimed to promote development of an innovative diagnostic procedure for diseases with major public health importance.

**Institutional Review Board Statement:** Not applicable.

**Informed Consent Statement:** Not applicable.

**Data Availability Statement:** All data generated or analyzed during this study are included in this published article (and its Supplementary Information files) or are available from the corresponding author upon reasonable request.

**Conflicts of Interest:** The authors declare no conflicts of interest.

## References

1. Klymchenko, A.S.; Mely, Y. Fluorescent Environment-Sensitive Dyes as Reporters of Biomolecular Interactions. In *Fluorescence-Based Biosensors—From Concepts to Applications*; Academic Press: Cambridge, MA, USA, 2013; pp. 35–58.
2. Reichardt, C. Solvatochromic Dyes as Solvent Polarity Indicators. *Chem. Rev.* **2002**, *94*, 2319–2358. [[CrossRef](#)]
3. Pal, K.; Dutta, T.; Koner, A.L. An Enumerated Outlook of Intracellular Micropolarity Using Solvatochromic Organic Fluorescent Probes. *ACS Omega* **2020**, *6*, 28–37. [[CrossRef](#)] [[PubMed](#)]
4. Hickey, S.M.; Johnson, I.R.D.; Dallerba, E.; Hackett, M.J.; Massi, M.; Lazniewska, J.; Thurgood, L.A.; Pfeffer, F.M.; Brooks, D.A.; Ashton, T.D. A fluorescent and solvatochromic 1,8-naphthalimide probe for detection of lipid droplet trafficking and biogenesis. *Dyes Pigments* **2023**, *217*, 111382. [[CrossRef](#)]
5. Marini, A.; Muñoz-Losa, A.; Biancardi, A.; Mennucci, B. What is Solvatochromism? *J. Phys. Chem. B* **2010**, *114*, 17128–17135. [[CrossRef](#)]
6. Weber, G.; Farris, F.J. Synthesis and spectral properties of a hydrophobic fluorescent probe: 6-propionyl-2-(dimethylamino)naphthalene. *Biochemistry* **1979**, *18*, 3075–3078. [[CrossRef](#)]
7. Rácz, D.; Nagy, M.; Mándi, A.; Zsuga, M.; Kéki, S. Solvatochromic properties of a new isocyanonaphthalene based fluorophore. *J. Photochem. Photobiol. A Chem.* **2013**, *270*, 19–27. [[CrossRef](#)]
8. Nagy, M.; Rácz, D.; Nagy, Z.L.; Fehér, P.P.; Kalmár, J.; Fábrián, I.; Kiss, A.; Zsuga, M.; Kéki, S. Solvatochromic isocyanonaphthalene dyes as ligands for silver(I) complexes, their applicability in silver(I) detection and background reduction in biolabelling. *Sens. Actuators B Chem.* **2018**, *255*, 2555–2567. [[CrossRef](#)]

9. Nagy, M.; Kovács, S.L.; Nagy, T.; Rácz, D.; Zsuga, M.; Kéki, S. Isocyanonaphthalenes as extremely low molecular weight, selective, ratiometric fluorescent probes for Mercury(II). *Talanta* **2019**, *201*, 165–173. [[CrossRef](#)]
10. Abelt, C.J.; Sun, T.; Everett, R.K. 2,5-PRODAN: Synthesis and properties. *Photochem. Photobiol. Sci.* **2020**, *10*, 618–622. [[CrossRef](#)]
11. Davis, B.N.; Abelt, C.J. Synthesis and photophysical properties of models for twisted PRODAN and dimethylaminonaphthonitrile. *J. Phys. Chem. A* **2005**, *109*, 1295–1298. [[CrossRef](#)]
12. Yee, D.J.; Balsanek, V.; Sames, D. New Tools for Molecular Imaging of Redox Metabolism: Development of a Fluorogenic Probe for  $3\alpha$ -Hydroxysteroid Dehydrogenases. *J. Am. Chem. Soc.* **2004**, *126*, 2282–2283. [[CrossRef](#)] [[PubMed](#)]
13. Jockusch, S.; Zheng, Q.; He, G.S.; Pudavar, H.E.; Yee, D.J.; Balsanek, V.; Halim, M.; Sames, D.; Prasad, P.N.; Turro, N.J. Two-Photon Excitation of Fluorogenic Probes for Redox Metabolism: Dramatic Enhancement of Optical Contrast Ratio by Two-Photon Excitation. *J. Phys. Chem. C* **2007**, *111*, 8872–8877. [[CrossRef](#)]
14. Niko, Y.; Kawauchi, S.; Konishi, G.-I. Solvatochromic Pyrene Analogues of Prodan Exhibiting Extremely High Fluorescence Quantum Yields in Apolar and Polar Solvents. *Chem. Eur. J.* **2013**, *19*, 9760–9765. [[CrossRef](#)]
15. Nagy, M.; Fiser, B.; Szőri, M.; Vanyorek, L.; Viskolcz, B. Optical Study of Solvatochromic Isocyanaminoanthracene Dyes and 1,5-Diaminoanthracene. *Int. J. Mol. Sci.* **2022**, *23*, 1315. [[CrossRef](#)] [[PubMed](#)]
16. Lu, Z.; Lord, S.J.; Wang, H.; Moerner, W.E.; Twieg, R.J. Long-Wavelength Analogue of PRODAN: Synthesis and Properties of Anthradan, a Fluorophore with a 2,6-Donor-Acceptor Anthracene Structure. *J. Org. Chem.* **2006**, *71*, 9651–9657. [[CrossRef](#)] [[PubMed](#)]
17. Bankó, C.; Nagy, Z.L.; Nagy, M.; Szemán-Nagy, G.G.; Rebenku, I.; Imre, L.; Tiba, A.; Hajdu, A.; Szöllősi, J.; Kéki, S.; et al. Isocyanide Substitution in Acridine Orange Shifts DNA Damage-Mediated Phototoxicity to Permeabilization of the Lysosomal Membrane in Cancer Cells. *Cancers* **2021**, *13*, 5652. [[CrossRef](#)] [[PubMed](#)]
18. Nagy, M.; Rácz, D.; Kovács, S.L.; Lázár, L.; Fehér, P.P.; Purgel, M.; Zsuga, M.; Kéki, S. New blue light-emitting isocyanobiphenyl based fluorophores: Their solvatochromic and biolabeling properties. *J. Photochem. Photobiol. A Chem.* **2016**, *318*, 124–134. [[CrossRef](#)]
19. Fang, Q.; Xu, B.; Jiang, B.; Fu, H.; Zhu, W.; Jiang, X.; Zhang, Z. A novel fluorene derivative containing four triphenylamine groups: Highly thermostable blue emitter with hole-transporting ability for organic light-emitting diode (OLED). *Synth. Met.* **2005**, *155*, 206–210. [[CrossRef](#)]
20. Orofino, C.; Foucher, C.; Farrell, F.; Findlay, N.J.; Breig, B.; Kanibolotsky, A.L.; Guilhabert, B.; Vilela, F.; Laurand, N.; Dawson, M.D.; et al. Fluorene-containing tetraphenylethylene molecules as lasing materials. *J. Polym. Sci. Part A Polym. Chem.* **2016**, *55*, 734–746. [[CrossRef](#)]
21. Lasne, M.-C.; Perrio, C.; Rouden, J.; Barré, L.; Roeda, D.; Dolle, F.; Crouzel, C. Chemistry of  $\beta$  +-Emitting Compounds Based on Fluorine-18. In *Contrast Agents II*; Springer: Berlin/Heidelberg, Germany, 2002; pp. 201–258.
22. Chen, Z.; Liang, J.; Han, X.; Yin, J.; Yu, G.-A.; Liu, S.H. Fluorene-based novel highly emissive fluorescent molecules with aggregate fluorescence change or aggregation-induced emission enhancement characteristics. *Dyes Pigments* **2015**, *112*, 59–66. [[CrossRef](#)]
23. Kucherak, O.A.; Didier, P.; Mély, Y.; Klymchenko, A.S. Fluorene Analogues of Prodan with Superior Fluorescence Brightness and Solvatochromism. *J. Phys. Chem. Lett.* **2010**, *1*, 616–620. [[CrossRef](#)]
24. Karunakaran, V.; Senyushkina, T.; Saroja, G.; Liebscher, J.; Ernsting, N.P. 2-Amino-7-nitro-fluorenes in Neat and Mixed Solvents Optical Band Shapes and Solvatochromism. *J. Phys. Chem. A* **2007**, *111*, 10944–10952. [[CrossRef](#)]
25. Fallon, L.; Ammon, H.L. Crystal and molecular structures of 2'-nitro-4-aminobiphenyl and 2-amino-7-nitrofluorene. *J. Cryst. Mol. Struct.* **1974**, *4*, 63–75. [[CrossRef](#)]
26. Ritter, C.L.; Culp, S.J.; Freeman, J.P.; Marques, M.M.; Beland, F.A.; Malejka-Giganti, D. DNA Adducts from Nitroreduction of 2,7-Dinitrofluorene, a Mammary Gland Carcinogen, Catalyzed by Rat Liver or Mammary Gland Cytosol. *Chem. Res. Toxicol.* **2002**, *15*, 536–544. [[CrossRef](#)]
27. Nawara, K.; Waluk, J. Goodbye to Quinine in Sulfuric Acid Solutions as a Fluorescence Quantum Yield Standard. *Anal. Chem.* **2019**, *91*, 5389–5394. [[CrossRef](#)] [[PubMed](#)]
28. Frisch, M.J.; Trucks, G.W.; Schlegel, H.B.; Scuseria, G.E.; Robb, M.A.; Cheeseman, J.R.; Scalmani, G.; Barone, V.; Petersson, G.A.; Nakatsuji, H.; et al. *Gaussian 16 Rev. C.01*; Gaussian Inc.: Wallingford, CT, USA, 2016.
29. Zhao, Y.; Truhlar, D.G. The M06 suite of density functionals for main group thermochemistry, thermochemical kinetics, noncovalent interactions, excited states, and transition elements: Two new functionals and systematic testing of four M06-class functionals and 12 other functionals. *Theor. Chem. Acc.* **2007**, *120*, 215–241.
30. Becke, A.D. Density-functional thermochemistry. III. The role of exact exchange. *J. Chem. Phys.* **1993**, *98*, 5648–5652. [[CrossRef](#)]
31. Tomasi, J.; Mennucci, B.; Cammi, R. Quantum Mechanical Continuum Solvation Models. *Chem. Rev.* **2005**, *105*, 2999–3094. [[CrossRef](#)] [[PubMed](#)]
32. Catalán, J. Toward a Generalized Treatment of the Solvent Effect Based on Four Empirical Scales: Dipolarity (SdP, a New Scale), Polarizability (SP), Acidity (SA), and Basicity (SB) of the Medium. *J. Phys. Chem. B* **2009**, *113*, 5951–5960. [[CrossRef](#)] [[PubMed](#)]
33. Allen, F.H.; Kennard, O.; Watson, D.G.; Brammer, L.; Orpen, A.G.; Taylor, R. Tables of bond lengths determined by X-ray and neutron diffraction. Part 1. Bond lengths in organic compounds. *J. Chem. Soc. Perkin Trans. 2* **1987**, *12*, S1–S19. [[CrossRef](#)]
34. Schleyer, P.V.R.; Maerker, C.; Dransfeld, A.; Jiao, H.; van Eikema Hommes, N.J.R. Nucleus-Independent Chemical Shifts: A Simple and Efficient Aromaticity Probe. *J. Am. Chem. Soc.* **1996**, *118*, 6317–6318. [[CrossRef](#)] [[PubMed](#)]

- 
35. Mucsi, Z.; Viskolcz, B.; Csizmadia, I.G. A Quantitative Scale for the Degree of Aromaticity and Antiaromaticity: A Comparison of Theoretical and Experimental Enthalpies of Hydrogenation. *J. Phys. Chem. A* **2007**, *111*, 1123–1132. [[CrossRef](#)] [[PubMed](#)]
  36. Héder, M.; Rigó, E.; Medgyesi, D.; Lovas, R.; Tenczer, S.; Török, F.; Farkas, A.; Emődi, M.; Kadlecik, J.; Mező, G.; et al. The Past, Present and Future of the ELKH Cloud. *Információs Társadalom* **2022**, *22*, 128–137. [[CrossRef](#)]

**Disclaimer/Publisher’s Note:** The statements, opinions and data contained in all publications are solely those of the individual author(s) and contributor(s) and not of MDPI and/or the editor(s). MDPI and/or the editor(s) disclaim responsibility for any injury to people or property resulting from any ideas, methods, instructions or products referred to in the content.